

Article

“Realistic Choice of Annual Matrices Contracts the Range of λ_S Estimates” under Reproductive Uncertainty Too

Dmitrii O. Logofet ^{1,*} , Leonid L. Golubyatnikov ¹ , Elena S. Kazantseva ² and Nina G. Ulanova ² 

¹ Laboratory of Mathematical Ecology, A.M. Obukhov Institute of Atmospheric Physics, Russian Academy of Sciences, 119017 Moscow, Russia; golub@ifaran.ru

² Biological Department, Moscow State University, 119234 Moscow, Russia; biolenok@mail.ru (E.S.K.); nulanova@mail.ru (N.G.U.)

* Correspondence: danilal@postman.ru

Abstract: Our study is devoted to a subject popular in the field of matrix population models, namely, estimating the *stochastic growth rate*, λ_S , a quantitative measure of long-term population viability, for a discrete-stage-structured population monitored during many years. “*Reproductive uncertainty*” refers to a feature inherent in the data and *life cycle graph* (LCG) when the LCG has more than one reproductive stage, but when the progeny cannot be associated to a parent stage in a unique way. Reproductive uncertainty complicates the procedure of λ_S estimation following the defining of λ_S from the limit of a sequence consisting of population projection matrices (PPMs) chosen randomly from a given set of annual PPMs. To construct a Markov chain that governs the choice of PPMs for a local population of *Eritrichium caucasicum*, an short-lived perennial alpine plant species, we have found a local weather index that is correlated with the variations in the annual PPMs, and we considered its long time series as a realization of the Markov chain that was to be constructed. Reproductive uncertainty has required a proper modification of how to restore the transition matrix from a long realization of the chain, and the restored matrix has been governing random choice in several series of Monte Carlo simulations of long-enough sequences. The resulting ranges of λ_S estimates turn out to be more narrow than those obtained by the popular *i.i.d.* methods of random choice (independent and identically distributed matrices); hence, we receive a more accurate and reliable forecast of population viability.

Keywords: discrete-structured population; matrix population model; population projection matrices; reproductive uncertainty; stochastic growth rate; random choice; weather indices; Markov chain; Monte Carlo simulations



Citation: Logofet, D.O.; Golubyatnikov, L.L.; Kazantseva, E.S.; Ulanova, N.G. “Realistic Choice of Annual Matrices Contracts the Range of λ_S Estimates” under Reproductive Uncertainty Too. *Mathematics* **2021**, *9*, 3007. <https://doi.org/10.3390/math9233007>

Academic Editor: Åke Brännström

Received: 27 October 2021

Accepted: 22 November 2021

Published: 24 November 2021

Publisher’s Note: MDPI stays neutral with regard to jurisdictional claims in published maps and institutional affiliations.



Copyright: © 2021 by the authors. Licensee MDPI, Basel, Switzerland. This article is an open access article distributed under the terms and conditions of the Creative Commons Attribution (CC BY) license (<https://creativecommons.org/licenses/by/4.0/>).

1. Introduction

The citation in the title is taken from that of the former publication [1] devoted to the estimation of λ_S , in which the stochastic growth rate of a population was calculated in the framework of a matrix population model (MPM, [2]).

The mathematical demography of plant and animal populations is at present based mostly on MPMs as basic research tools [2] for organizing data gained by the observations/measurements of the population structure, $x(t) \in \mathbb{R}_+^n$, with regard to a certain classification trait, e.g., age, size, or the stage of ontogenesis [2] in the individuals of a local population of a given species. In mathematical terms, the MPM is a system of difference equations,

$$x(t+1) = L(t)x(t), \quad t = 0, 1, 2, \dots, \quad (1)$$

for the n -vector of a *population structure* that belongs to the positive orthant of the n -dimensional Euclidean space. Matrix $L(t)$ is non-negative and called the *population projection matrix* (PPM) [2,3]: “Each component of $x(t)$ is the (absolute or relative) number of individuals in the corresponding status-specific group at time moment t , while the elements

of $L(t)$, called *vital rates* [2], carry information about the rates of demographic processes in the population. They are time-dependent in general, but the zero-nonzero pattern of the PPM corresponds invariably to a single *associated directed graph* [4], which is called the *life cycle graph* [2] (LCG) as a condensed graphical representation of the biological knowledge involved into the model and the way the population structure is observed in the study” ([1], p. 1) (see the next Section for a sample).

When $L(t) = L$ does not change in time, the dynamics of $x(t)$ as $t \rightarrow \infty$ is provided by the classical Perron–Frobenius Theorem for non-negative irreducible matrices [4]. By the Theorem, the spectrum of L contains a simple eigenvalue, $\lambda_1 > 0$, that is positive and equal to the spectral radius, $\rho(L)$, of the matrix; this eigenvalue is called *dominant*. There also exists a positive eigenvector, $x^* > 0$, corresponding to the dominant eigenvalue. It follows that, when matrix L is *primitive*, the sequence of $x(t)/\lambda_1^t$ converges to a vector proportional to x^* for any nonzero $x(0) \geq 0$ [4,5] and to a periodic vector function of t when L is imprimitive [5]. Clearly, the population declines when $\lambda_1(L) < 1$, and it grows exponentially when $\lambda_1(L) > 1$, so that $\lambda_1(L)$ represents the *asymptotic growth rate*.

In applications, $\lambda_1(L)$ measures “the adaptation that the local population possessed in the place where, and at the time when, the population data were collected to calibrate the matrix L ” ([6], p. 176; [7]). Two successive years of observation are typically sufficient to calibrate $L(t)$, the *annual PPM*, in a unique way [1], although situations occur where the reproduction rates can only be determined up to a bounded positive parameter [8,9]; we call this *reproductive uncertainty* [10] since the calibrating equation (1) is satisfied for any feasible values of the reproduction rates. As a result, we obtain a finite range of possible λ_1 values, rather than a single value for a uniquely calibrated $L(t)$.

In both cases however, more than two observation years provide, respectively, more than two annual PPMs with values ([11], Table 3) or ranges ([12], Table 3) of λ_1 that differ both quantitatively and *qualitatively* (less or greater than 1). The task is therefore to assess the state of a population from multi-year observation data; hence, a finite set of annual PPMs, and λ_S , the *stochastic growth rate* [2,13], provides for such an assessment. A variety of methods is known to estimate λ_S for a given set of annual PPMs (see a survey in [2]), but we have proposed an original method [1], which related (for the first time to our knowledge) the estimation of λ_S to the variations in local meteorological data. This new method has resulted in more accurate estimates of λ_S than another popular method also applicable to the population data in hand has done previously [1].

With the purpose to develop our method further, we expose it, in the next section, with an emphasis on the reproductive uncertainty feature of the population data gained in a case study of *Eritrichium caucasicum*, a short-lived perennial alpine plant species. Reproductive uncertainty in observation data causes certain sets of annual PPMs, instead of single matrices, that are calibrated from data, and we modify the successive steps of our procedure to reconstruct a governing Markov chain that is related to variations in the environment. The “Results” section contains the outcome of comparing our estimates of λ_S to those obtained by the so-called “i.i.d.” rules of random choice (independent and identically distributed matrices, [2]). In the final section, we discuss the novelty of our method caused by the reproductive uncertainty and what might follow from our current findings for the Red Data Book status of *E. caucasicum*.

In Table 1, we enlist the abbreviations and formal notations used throughout the text.

Table 1. List of abbreviations and formal notations used throughout the text ¹.

Abbreviations and Notations	Meaning
LCG	Life Cycle Graph
PPM	Population Projection Matrix
i.i.d.	Independent, identically distributed
MPM	Matrix Population Model
MC	Monte Carlo
$x(t)$	Vector of population structure
$j(t), v(t), g(t), gt(t)$	Components of $x(t)$ for <i>Eritrichium caucasicum</i>
$a(t), b(t)$	Uncertain fertility rates for <i>E. caucasicum</i> at time t
\mathbb{R}_+^n	Positive orthant of the n -dimension vector space
$L(t)$	PPM at time t
$L(t; a)$	PPM at time t for parameter value a
$\{L(t; a)\}$	A set of PPMs at time t for all feasible values of a
$\lambda_1(L)$	Dominant eigenvalue of matrix L
$\rho(L)$	Spectral radius of matrix L
$\lambda_1(t; a)$	Dominant eigenvalue of matrix $L(t; a)$
$\Lambda(t; a)$	A set of $\lambda_1(t; a)$ s at time t for all feasible values of a
$\lambda_{1\min}, \lambda_{1\max}$	The minimal and maximal values of λ_1 over a set Λ
x^*	Positive eigenvector corresponding to $\lambda_1(L)$
λ_S	The stochastic growth rate
$P = [p_{ij}]$	Markov chain transition matrix and its elements
ss^*	Steady-state distribution of Markov chain states
$\theta(t)$	Observed time series of the temperature index, θ

¹ Except for those standard in the statistical treatment of data.

2. Materials and Methods

2.1. Case Study of *Eritrichium Caucasicum*

Eritrichium caucasicum (Albov) Grossh. is a short-lived herbaceous perennial polycarpic plant species that is endemic to Caucasus and that inhabits alpine heaths. We described the biology, ecology, and ontogenesis of the species (Figure 1) in earlier publications [8,14], and the corresponding LCG was developed (Figure 2).



Figure 1. Ontogenetic stages of *Eritrichium caucasicum*: pl, seedlings; j, juvenile plants; v, adult vegetative plants; g, generative plants; gt, terminal generative plants, the stages being distinguishable in the field [8].

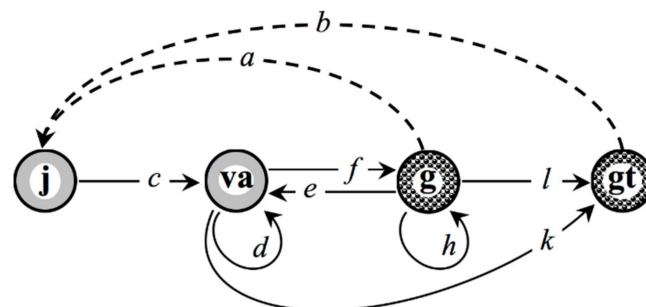


Figure 2. LCG for a local population of *Eritrichium caucasicum* observed once a year. Ontogenetic stage notations as in Figure 1. Solid arrows indicate transitions occurring for one year (no transitions, in particular); dashed arrows correspond to annual recruitments [12].

The *stage structure*, i.e., vector $x(t) = [j(t), v(t), g(t), gt(t)]^T$, of a local *E. caucasicum* population has been annually observed on permanent plots laid down on the Malaya Khatipara mountain (2800 m asl., Teberda State Nature Reserve, north-western Caucasus) in 2009 [8]; the observation has been done at the end of growing season, every August for, now, a total of 12 years (2009–2020). Each individual plant was marked and its fate was traced through years, so that the observation data are of the “identified individuals” type [2], enabling, also, the record of each transition between stages and each recruited individual.

Stage j incorporates seedlings pl as they transition to juveniles quite quickly, within a single growing season. Along with successive transitions from stage to stage for one year, the following events were also observed in the *E. caucasicum* life history:

- delays \circ in stages va and g, which can be explained by the harsh conditions of the highlands [15]. Some virginal plants also accumulate resources for fruiting longer than one year because of soil poorness [16–19];
- returns $va \leftarrow g$ because of adverse climatic conditions and insufficiency of a single growing season for a generative plant to accumulate resources for fruiting [15,20,21];

- accelerated transitions $\mathbf{va} \curvearrowright \mathbf{gt}$ as a manifestation of polyvariant ontogeny in *E. caucasicum* under the conditions of the alpine belt in north-western Caucasus.

Two generative stages provide for the population recruitment, the new individuals being observed at stage j (Figure 2). However, the stage of their parent plants cannot, unfortunately, be determined, and this is a fundamental reason for what we call *reproductive uncertainty* [10,12]. The corresponding scalar equation of system (1) for $\mathbf{x}(t) = [j(t), v(t), g(t), gt(t)]^T$ thus takes on the following form:

$$j(t + 1) = a(t)g(t) + b(t)gt(t), t = 2009, 2010, \dots, 2019, \tag{2}$$

for the unknowns $a(t)$ and $b(t)$. The left-hand side and coefficients of Equation (2) are integers, whereby the solution to this Diophantine equation represents a finite set of rational numbers expressed in terms of, say, parameter a . As a result of 12 observation years under reproductive uncertainty, we obtain 11 finite sets, $\{L(t; a)\}$, of annual PPMs shown in Table 2. Correspondingly, their λ_1 constitute 11 finite sets, $\Lambda(t; a) \ni \lambda_1(t; a)$, with their minimal and maximal values at the boundary values of a .

Table 2. One-parameter sets of annual PPMs $L(t; a)$ calibrated from the *E. caucasicum* data at the years $t, t + 1$ and the corresponding bounds of λ_1 (modification and expansion of Table 3 from [12]).

t $i = t - 2008$	Matrix $L(t; a) = L_i(a)$	Recruitment Equation; $\{a \text{ Values}\}$ $a^\circ, \lambda_1(a^\circ)^1$	Range of $\lambda_1(L(t))$	
			$\lambda_{1\min}$	$\lambda_{1\max}$
2009 1	$\begin{bmatrix} 0 & 0 & a & \frac{31-10a}{4} \\ \frac{68}{149} & \frac{63}{80} & \frac{5}{10} & 0 \\ 0 & \frac{6}{80} & \frac{3}{10} & 0 \\ 0 & 0 & \frac{1}{10} & 0 \end{bmatrix}$	$\begin{aligned} &10a + 4b = 31; \\ &\{0, \frac{1}{10}, \frac{2}{10}, \dots, \frac{31}{10}\} \\ &\frac{14}{10}, 0.948257 \end{aligned}$	0.9035	0.9949
2010 2	$\begin{bmatrix} 0 & 0 & a & \frac{150-9a}{1} \\ \frac{17}{31} & \frac{106}{136} & \frac{6}{9} & 0 \\ 0 & \frac{136}{9} & \frac{1}{9} & 0 \\ 0 & \frac{2}{136} & \frac{1}{9} & 0 \end{bmatrix}$	$\begin{aligned} &9a + b = 150; \\ &\{0, \frac{1}{9}, \frac{2}{9}, \dots, \frac{150}{9}\} \\ &\frac{87}{9}, 1.383299 \end{aligned}$	1.2460	1.5201
2011 3	$\begin{bmatrix} 0 & 0 & a & \frac{211-10a}{3} \\ \frac{76}{150} & \frac{101}{129} & \frac{4}{10} & 0 \\ 0 & \frac{129}{4} & \frac{2}{10} & 0 \\ 0 & \frac{4}{129} & \frac{3}{10} & 0 \end{bmatrix}$	$\begin{aligned} &10a + 3b = 211; \\ &\{0, \frac{1}{10}, \frac{2}{10}, \dots, \frac{211}{10}\} \\ &\frac{121}{10}, 1.371439 \end{aligned}$	1.2476	1.4948
2012 4	$\begin{bmatrix} 0 & 0 & a & \frac{119-9a}{7} \\ \frac{137}{211} & \frac{153}{181} & \frac{6}{9} & 0 \\ 0 & \frac{6}{181} & \frac{0}{9} & 0 \\ 0 & 0 & \frac{1}{9} & 0 \end{bmatrix}$	$\begin{aligned} &9a + 7b = 119; \\ &\{0, \frac{1}{9}, \frac{2}{9}, \dots, \frac{119}{9}\} \\ &\frac{52}{9}, 1.010985 \end{aligned}$	0.9213	1.1004
2013 5	$\begin{bmatrix} 0 & 0 & a & \frac{99-6a}{1} \\ \frac{23}{119} & \frac{139}{296} & \frac{4}{6} & 0 \\ 0 & \frac{9}{296} & \frac{2}{6} & 0 \\ 0 & \frac{4}{296} & \frac{0}{6} & 0 \end{bmatrix}$	$\begin{aligned} &6a + b = 99; \\ &\{0, \frac{1}{6}, \frac{2}{6}, \dots, \frac{99}{6}\} \\ &\frac{49}{6}, 0.822941 \end{aligned}$	0.7864	0.8588
2014 6	$\begin{bmatrix} 0 & 0 & a & \frac{49-11a}{4} \\ \frac{22}{99} & \frac{103}{166} & \frac{3}{11} & 0 \\ 0 & \frac{14}{166} & \frac{3}{11} & 0 \\ 0 & \frac{3}{166} & \frac{5}{11} & 0 \end{bmatrix}$	$\begin{aligned} &11a + 4b = 49; \\ &\{0, \frac{1}{11}, \frac{2}{11}, \dots, \frac{49}{11}\} \\ &\frac{28}{11}, 0.874279 \end{aligned}$	0.8376	0.9119

Table 2. Cont.

t $i = t - 2008$	Matrix $L(t; a) = L_i(a)$	Recruitment Equation; $\{a \text{ Values}\}$ $a^\circ, \lambda_1(a^\circ)^1$	Range of $\lambda_1(L(t))$	
			$\lambda_{1\min}$	$\lambda_{1\max}$
2015 7	$\begin{bmatrix} 0 & 0 & a & \frac{73-17a}{8} \\ \frac{9}{49} & \frac{86}{128} & \frac{8}{17} & 0 \\ 0 & 0 & \frac{1}{17} & 0 \\ 0 & \frac{1}{128} & \frac{1}{17} & 0 \\ 0 & \frac{1}{128} & \frac{1}{17} & 0 \end{bmatrix}$	$17a + 8b = 73;$ $\{0, \frac{1}{17}, \frac{2}{17}, \dots, \frac{73}{17}\}$ $\frac{38}{17}, 0.685245$	0.6719	0.6987
2016 8	$\begin{bmatrix} 0 & 0 & a & \frac{13-a}{1} \\ \frac{15}{73} & \frac{60}{103} & \frac{0}{1} & 0 \\ 0 & \frac{5}{103} & \frac{0}{1} & 0 \\ 0 & \frac{1}{103} & \frac{0}{1} & 0 \\ 0 & \frac{1}{103} & \frac{0}{1} & 0 \end{bmatrix}$	$a + b = 13;$ $\{0, 1, 2, \dots, 13\}$ $5, 0.712283$	0.6449	0.7902
2017 9	$\begin{bmatrix} 0 & 0 & a & \frac{49-5a}{1} \\ \frac{5}{13} & \frac{58}{75} & \frac{3}{5} & 0 \\ 0 & \frac{2}{75} & \frac{1}{5} & 0 \\ 0 & \frac{0}{75} & \frac{1}{5} & 0 \\ 0 & \frac{0}{75} & \frac{1}{5} & 0 \end{bmatrix}$	$5a + b = 49;$ $\{0, \frac{1}{5}, \frac{2}{5}, \dots, \frac{49}{5}\}$ $\frac{26}{5}, 0.942585$	0.9396	0.9456
2018 10	$\begin{bmatrix} 0 & 0 & a & \frac{72-3a}{1} \\ \frac{2}{49} & \frac{40}{66} & \frac{0}{3} & 0 \\ 0 & \frac{0}{66} & \frac{0}{3} & 0 \\ 0 & \frac{1}{66} & \frac{0}{3} & 0 \\ 0 & \frac{1}{66} & \frac{0}{3} & 0 \end{bmatrix}$	$3a + b = 72;$ $\{0, \frac{1}{3}, \frac{2}{3}, \dots, \frac{72}{3}\}$ $\frac{41}{3}, 0.651261$	0.6061	0.6976
2019 11	$\begin{bmatrix} 0 & 0 & a & 7 - a \\ \frac{31}{72} & \frac{14}{42} & \frac{0}{1} & 0 \\ 0 & \frac{12}{42} & \frac{0}{1} & 0 \\ 0 & \frac{4}{42} & \frac{0}{1} & 0 \\ 0 & \frac{1}{42} & \frac{0}{1} & 0 \end{bmatrix}$	$a + b = 7;$ $\{0, 1, 2, \dots, 7\}$ $2, 1.237478$	1.0000	1.4955

¹ Nearest to the average of λ_1 : $\lambda_1(a^\circ) = \min_a |\lambda_1(a) - (\lambda_{1\min} + \lambda_{1\max})/2|$.

In spite of reproductive uncertainty, all of (a finite number of) the $\lambda_1(L(t; a))$ values, except for $t = 2012$, are qualitatively certain: either less or greater than 1, $1 \notin \Lambda(t; a)$. Nevertheless, the final outcome of the 12-year monitoring of population states remains uncertain, while the certainty can be reached in the paradigm of the stochastic growth rate.

2.2. Stochastic Growth Rate, λ_S

The idea of the stochastic growth rate ensues from the paradigm of population dynamics in a stochastic environment ([2] and the references therein). Given a set of annual PPMs, each of them is considered to correspond to a state of the environment that would provide for either further exponential growth or decline of the population if the state did not change. The *stochastic environment* is thereafter considered as a sequence of PPMs chosen at random from the given set [2]. Each of the PPMs projects the current population vector for one step further, and the sequence of total population sizes ($\|\dots\|_1$) converges, under unrestrictive technical conditions, to a finite limit

$$\lim_{\tau \rightarrow \infty} \frac{1}{\tau} \ln N(\tau) = \lim_{\tau \rightarrow \infty} \frac{1}{\tau} \ln \|L_{\tau-1} \dots L_0\|_1 = \ln \lambda_S \tag{3}$$

with probability 1 [22–24]. The value of λ_S is then called the *stochastic growth rate*, and we concentrate our efforts on how to estimate the limit (3) when a set of calibrated annual PPMs is available together with their λ_1 s.

Known from the literature, theoretical estimates of λ_S [2,13] suggest certain assumptions about the set of $L(t)$ s, such as, e.g., their distribution around an average matrix with a known variance. However, when the given PPMs differ dramatically from one another (Table 1, see also [11,12]), we have just to resort to definition (3). The well-known Monte

Carlo (MC) method prompts the way of constructing a finite piece of the infinite sequence once a rule for the random choice of matrices at each step τ has been accepted. The simplest and most popular rule is reduced to the *independent, identically distributed* (i.i.d.) matrices, and we obtain a set of random realizations of sequence (3) and the corresponding range of λ_S estimates over the set [12].

However, the i.i.d. matrices can hardly be accepted as an adequate model of real stochastic environments, where the population vital rates (elements of PPMs) would rather react to variations in the environment than obey any i.i.d. rule, while the variations themselves are caused by changing weather or other factors. A step towards reality was associated with Markov chains [25], which have become a popular tool in present-day weather modeling [26–28]. Markov chains were also suggested to govern the random choice of PPMs in the paradigm of λ_S [24,29], and they are used for both theoretical and practical estimations of λ_S , “varying from very simple, such as switching between ‘bad’ and ‘good’ environments [30], to highly sophisticated ones [31–33], yet still invented by the authors rather than by nature” ([1], p. 2/15).

On the contrary, we have already constructed a Markov chain that describes those real variations in the environment of a local population that were indirectly expressed in a given set of 10 annual PPMs, yet without reproductive uncertainty [1]. Neither the graph of transitions nor the transition *probabilities* were known a priori, and the task was to reconstruct the graph and to estimate the probabilities, thus obtaining the *transition matrix*, $\mathbf{P} = (p_{ij})$, from a variety of local meteorological and microphysical data that scoped 59 observation years. Constructed in this way, matrix \mathbf{P} enabled us to obtain more narrow, hence more accurate, ranges of λ_S estimates (Table 4 in [1]) than those obtained before under the i.i.d. *equiprobable* matrices (Table 6 in [34]); a less trivial i.i.d. choice still generated worse estimates (Table 4 in [1]).

The challenge is now to develop our method for the case of reproductive uncertainty, and further sections report our response to this challenge.

2.3. Local Meteodata, Statistical Treatment

Along with the monitoring of the local *E. caucasicum* population, certain climatic parameters at the site (an alpine heath), close to the permanent plots under study, were monitored. “From a variety of meteorological data on the air and soil registered by the local temperature/humidity sensors, we have selected certain key environmental factors effecting the population status and development, i.e., seed germination, seedling survival and growth, under severe conditions of the alpine belt. Twenty-one parameters were selected: the minimal, maximal, and average air temperatures in the previous-year autumn (September–October) and current-year spring plus early summer period (May–June); the soil surface and 10-cm depth temperatures in the previous-year autumn (September–October) and current-year spring plus early summer period (May–June); the duration of freezing on the soil surface and 10-cm depth during the winter period (the sum of the days when the maximal temperature was not exceeding -1 °C from the previous-year November to the current-year April); the daily average soil moisture pressure at the 10-cm soil depth during June, 17–30. The data on meteorological and soil indicators were collected by standard methods with automatic sensors” (p. 6/15 in [1]).

Additionally, the formerly developed database of 13 years (2007–2019) of observations at the Teberda State Meteorological Station (TSMS, the Karachay-Cherkess Republic, Russian Federation) accounting for 15 climatic indicators [1] has been updated with one more year of observations (2020). The database contains 15 ecologically sound indicators, which might reveal statistical relationships with the status and growth of the population under study, namely: “the average, minimal and maximal temperatures in the previous-year autumn (September and October); the minimum, maximum, and average temperatures in spring (May) and early summer (June); the amount of precipitation in the previous-year fall (September and October), the current-year spring to early summer period (May and

June), and the winter period (from the previous-year November to the current-year May)“ (p. 6/15 in [1]).

The task was to detect the factor (or factors) most correlated with the $\lambda_1(t; a^\circ)$ variations in time (Table 2), and we have developed a multiple regression model by the least-squares method (ordinary least squares). The number of factors to be analyzed significantly exceeds the number of observations, while three predictors at most could be included into the model. Therefore, we selected the factors by stepwise regression (forward regression). The distribution of $\lambda_1(t; a^\circ)$ as the dependent variable corresponds to the normal one ($p = 0.1420$ according to the Shapiro–Wilk test [35]). Whether the error distribution corresponds to the normal is assessed visually on the quantile-quantile graph.

The best regression models of the $\lambda_1(t; a^\circ)$ time series have been checked for autocorrelations under the condition that the incorporated factors were measured at all years of observation. To do so, two generalized linear models (function *gls* of the *nlme* package in the statistical environment R [36]) are built with and without level-1 autocorrelation (AR1) and compared to each other by means of the log-likelihood ratio (ANOVA function in R [37]).

As a result, any significant autocorrelations with a one-year lag have not been found ($p = 0.301$). The $\lambda_1(t; a^\circ)$ variable correlates positively with the average minimum air temperatures in May–June, and it turns out to be the only significant predictor in the models with one factor included: it explains 49.3% of the variance (Table S1 in Supplementary Materials). There is also a positive relationship between $\lambda_1(t; a^\circ)$ and the number of days with freezing at the soil level (*ibidem*), which explains 49.7% of the variance, but has a borderline significance ($p = 0.051$) because of a smaller number of years with data on soil freezing compared to the previous factor. The combination of these factors is also not significant and weakly increases the proportion of explained variance, compared to the model where there is only one factor of soil freezing (55.1%, $p = 0.135$). Moreover, it is impossible to simultaneously include these factors into the model since they are significantly correlated with each other (Spearman’s correlation coefficient $\rho = 0.824$, $p = 0.006$). Including other factors does not improve the model, nor does the introduction of the autocorrelation condition. Thus, none of the multiple regression models are found to be significant.

2.4. Revealing the Pattern of Transition Matrix and Estimating Its Elements

We are looking for a Markov chain to govern the random choice of a matrix from the given set of 11 sets $\{\{L_i(a)\}, i = 1, \dots, 11\}$, of annual PPMs (Table 2) in the construction of sequence (3), defining the stochastic growth rate, λ_S . The chain is supposed to follow the variations in the weather conditions that determine particular sets of vital rates for the local *E. caucasicum* population, in particular, the variations in a fairly long time series of the temperature index, $\theta(k)$, $k = 1960, \dots, 2019$. To do so, we have to associate each point of the series, $\theta(k)$, to a set, $\{\{L_i(a)\}$, of annual PPMs, or simply to its number i , $i = 1, 2, \dots, 11$, identified with the chain state. Thereafter, we consider the 60-member sequence of states as a realization of the Markov chain, and the task is to restore its transition matrix from this realization.

In order to obtain a longer-than-11 stochastic sequence of PPMs, we identify each of the 11 given PPM sets, $\{L(t; a)\}$, $t = 2009, \dots, 2019$, with the value of temperature index, $\theta(t)$, during the corresponding, $t \rightarrow t + 1$, period (see Section 2.3). All these sets are different (we call them *reference sets*); we number them with 1 to 11 in chronological order and use $\lambda_1(a^\circ)$ (Table 2) as a reference value. Climatic parameters, including the temperature one, $\theta(t)$, have, fortunately, been measured in the TSMS since the year of 1960, so that we have a 60-point time series. The task is thereafter to associate each successive point, $\theta(k)$, $k = 1960, \dots, 2019$, of that series to one of the 11 reference values, and we do so using the absolute difference, $|\theta(k) - \theta(t)|$, as a measure of distance, selecting the closest reference point:

$$t_{\text{next}} = t \in \{2009, \dots, 2019 \mid \theta(k) - \theta(t) = \min_t |\theta(k) - \theta(t)|\}. \quad (4)$$

When solving the minimization problem (4) at some successive steps of k , we have unfortunately faced the non-uniqueness (in fact, duality) of its solutions. For example, when $k = 1966$, we have

$$\min_t |\theta(1966) - \theta(t)| = 0.2 \tag{5}$$

(Table S2, Supplementary Materials), and this minimum is reached at two different values of t , namely,

$$\theta(1966) - \theta(2016) = -0.2 \tag{6}$$

$$\theta(1966) - \theta(2017) = +0.2$$

The information at this point is not sufficient to make a choice between 2016 and 2017, i.e., between $\{L_8(a)\}$ and $\{L_9(a)\}$, so we investigate what has happened at the previous step, $k - 1 = 1965$. In other words, we try to imagine our long time series as a realization of a 2nd-order Markov chain, where the probability distribution of transitions from the current state depends both on this state and the previous one. We see that the state at $k - 1 = 1965$ has been associated to $t = 2018$, i.e., the PPM set $\{L_{10}(a)\}$, with $\lambda_1(2018; a) < 1$ for each a (Table 2). Consequently, to promote the qualitative changeability of conditions at $k = 1966$, we have to choose, between the years 2016 and 2017, the one in which $\lambda_1(t; a) > 1$, or at least the max $\{\lambda_1(2016; a), \lambda_1(2017, a)\}$. This is obviously 2017 (Table 2), i.e., the transition at $k = 1966$ goes to $\{L_9(a)\}$. In the opposite case, when $k = 1997$, we have

$$\min_t |\theta(1997) - \theta(t)| = 0.5$$

(Table S2, Supplementary Materials), with

$$\theta(1997) - \theta(2015) = -0.5 \tag{7}$$

$$\theta(1997) - \theta(2011) = +0.5$$

and we investigate what happened at $k - 1 = 1996$. Since 1996 is associated with $\{L_2(a)\}$, with $\lambda_1(L_2(a)) > 1$, we choose, by symmetrical logic, the minimal from $\lambda_1(L_7(a))$ and $\lambda_1(L_3(a))$, namely, $\{L_7(a)\}$ with $\lambda_1(L_7(a)) < 1$.

In this way, we obtain a unique 60-member sequence of t -specific ($t = 2009, \dots, 2019$) PPM sets, which we consider as a realization of the Markov chain that will govern the choice of each next PPM in the sequence (3), defining λ_S . Thereafter, we restore a Markov chain from its realization by taking the frequency of each particular transition as the corresponding transition probability, thus forming the transition matrix, $P = (p_{ij})$, of the Markov chain. Its dominant (stochastic) eigenvector, ss^* , represents a *steady-state* distribution of the chain states [38], which can be used in the subsequent i.i.d. MC simulations (ss^* i.i.d.) for the purpose of comparison.

2.5. Estimating λ_S by the Direct MC Method with a Markov Chain

After the transition matrix, P , of the governing Markov chain has been found, we can construct a sequence of annual PPMs of any finite length in order to estimate λ_S according to definition (3). To provide for computer outputs being reproducible, we fix, as before [1], the initial population vector, $x(\tau = 0) = x(2009)$ (Table 1 in [1]) and the same set of PPMs, $\{L(2009; a)\}$ (Table 2), the limit (3) being independent of this choice [22–24]. However, the reproductive uncertainty causes a principal distinction from the former case already at this point, namely, at the random choice of a particular PPM, $L(2009; a)$, from the given set $\{L(2009; a)\}$. To do this choice, we first estimate the variance inherent in the set as

$$\sigma^2 = \frac{1}{M} \sum_1^M (a_k - a^\circ)^2 \tag{8}$$

where M denotes the set power (Table 2). Second, we sample a by a Box–Muller transformation method [39] from the normal distribution around a° , with the variance σ .

Obtained in this way, the first matrix in sequence (3) means the first column of the transition matrix P , as the distribution for the next MC choice of a matrix row i , hence a PPM set $\{L(t; a) \mid t = i + 2008\}$. Choosing a row i ($1 \leq i \leq 11$) is equivalent to tossing an imperfect 11-faced die with unequal face probabilities (the column of P ; see, e.g., Appendix A in [1]). The choice of a PPM from the set for the next term in sequence (3) is described in the previous paragraph. Now, putting $j = i$ determines the next column of P to govern the MC choice of the next t -specific set of PPMs, thereby a choice of a PPM from the set. Repeating this basic step provides a finite sequence (3) of any given length (technical details in Appendix A).

We use the same algorithm to obtain finite sequences (3) under the i.i.d. choice, as it represents a particular case of the Markov chain choice with the transition matrix P consisting of 11 identical columns. Those columns “give the desired distribution, hence the dice becoming perfect when the distribution is uniform” ([1], p. 8/15).

3. Results

3.1. Transition Matrix of the Governing Markov Chain

The procedure introduced in Section 2.4 results in the transition matrix $P = [p_{ij}]$ ($i, j = 1, 2, \dots, 11$) presented in Table 3. It is obviously column-stochastic. The steady-state distribution of chain states is given by ss^* , the dominant stochastic eigenvalue of matrix P .

Table 3. Transition matrix of the Markov chain governing the random choice of annual PPM sets and its dominant stochastic eigenvector.

Incoming States	Outgoing States											Eigenvec-tor, ss^*
	2009	2010	2011	2012	2013	2014	2015	2016	2017	2018	2019	
2009	8/22	2/6	2/4	0	0	0	4/7	3/6	2/4	0	1	0.385367
2010	4/22	0	0	0	0	0	1/7	0	0	0	0	0.086159
2011	2/22	1/6	0	0	0	0	0	1/6	0	0	0	0.066525
2012	0	0	1/4	0	0	0	0	0	0	0	0	0.016631
2013	0	0	0	1	0	0	0	0	0	2/4	0	0.048484
2014	0	0	0	0	1/3	0	0	0	0	0	0	0.016161
2015	1/22	2/6	0	0	0	1	1/7	1/6	1/4	0	0	0.112644
2016	4/22	0	1/4	0	0	0	1/7	0	0	0	0	0.102790
2017	2/22	0	0	0	0	0	0	1/6	0	1/4	0	0.068091
2018	0	1/6	0	0	2/3	0	0	0	1/4	0	0	0.063705
2019	1/22	0	0	0	0	0	0	0	0	1/4	0	0.033443
Column sum	1	1	1	1	1	1	1	1	1	1	1	1

Note that $P^6 > 0$, i.e., matrix P is irreducible [4], hence the recovered Markov chain is regular [38], providing for the existence of limit (3) [23,24] under the random choice governed by this chain. Further estimates of λ_S as a finite, distant enough member of sequence (3) are therefore well grounded.

3.2. Estimates of λ_S

Although the nature of finite sequences from definition (3) is random, the resulting λ_S estimates should follow certain regularities. From the real analysis of converging sequences, we know that the longer the sequence, the closer its final term is to the limit value. We apply the same design of MC experiments as before (Tables 4 and 6 in [34]; Table 4 in [1]) and expect a similar picture in what concerns the range of variations in the estimates obtained from the sequences of a fixed length under varying numbers of random realizations: the greater the number, the wider should be the range. Table 4 confirms these expectations. One thousand realizations of the 1-million long sequence in the Markov chain series give the most reliable estimation (green figures in Table 4).

Table 4. Estimates of the stochastic growth rate, λ_S , by the direct Monte Carlo technique ¹.

Product "Length"	Number of Realizations	Range of Variations in the Estimates of λ_S ; Range Length:		
		Markov Chain Series	i.i.d. Series	ss* i.i.d. Series
1×10^5	13	(0.920773, 0.923780) 0.0030069	(0.972350, 0.976529) 0.0041788	(0.941310, 0.943347) 0.0020375
	33	(0.920588, 0.923780) 0.0031915	(0.971819, 0.976529) 0.0047104	(0.940334, 0.944282) 0.0039485
	100	(0.920191, 0.923780) 0.0035883	(0.971202, 0.977042) 0.0058391	(0.940334, 0.944282) 0.0039485
2×10^5	13	(0.921190, 0.922904) 0.0017140	(0.972791, 0.974847) 0.0020564	(0.941034, 0.943227) 0.0021931
	33	(0.921071, 0.922904) 0.0018323	(0.972791, 0.975908) 0.0031171	(0.941034, 0.943227) 0.0021931
	100	(0.920568, 0.923068) 0.0024998	(0.972447, 0.975908) 0.0034615	(0.940959, 0.943427) 0.0024672
3×10^5	13	(0.921528, 0.922558) 0.0010302	(0.973440, 0.975091) 0.0016510	(0.941333, 0.942742) 0.0014095
	33	(0.921234, 0.922863) 0.0016290	(0.972836, 0.975091) 0.0022541	(0.941272, 0.942742) 0.0014701
	100	(0.921030, 0.922863) 0.0018331	(0.972359, 0.975091) 0.0027315	(0.940817, 0.942944) 0.0021265
5×10^5	13	(0.921215, 0.922159) 0.0009435	(0.973368, 0.974421) 0.0010530	(0.941407, 0.942535) 0.0011275
	33	(0.921215, 0.922447) 0.0012320	(0.972962, 0.974421) 0.0014588	(0.941183, 0.942535) 0.0013520
	100	(0.921215, 0.922741) 0.0015256	(0.972796, 0.974960) 0.0021640	(0.941082, 0.942820) 0.0017376
1×10^6	13	(0.921529, 0.922326) 0.0007971	(0.972836, 0.974286) 0.0014502	(0.941703, 0.942316) 0.0006123
	33	(0.921434, 0.922375) 0.0009410	(0.972836, 0.974336) 0.0015003	(0.941538, 0.942562) 0.0010235
	100	(0.921433, 0.922403) 0.0009697	(0.972836, 0.974572) 0.0017355	(0.941509, 0.942562) 0.0010530
	1000	(0.921158, 0.922505) 0.0013463	(0.972768, 0.974922) 0.0021542	(0.941256, 0.942702) 0.0014461

¹ Threshold value $z = 0.000021$, scaling factor $sf = 0.918400$ (see Appendix A).

As regards the expectation expressed in the paper title, it is also confirmed in the most reliable case: the range is smaller indeed than any one from two i.i.d. series.

4. Discussion

Although the *E. caucasicum* population reproduces by seeds, the stage of dormant seeds is deliberately not incorporated into the LCG (Figure 2), and certain grounds for that have been intensively discussed ([40]; see Section 4 in [1] and references therein).

The reproductive uncertainty feature of the *E. caucasicum* data and the ensuing LCG cannot be avoided by aggregating two reproducing stages, **g** and **gt**, into a single one: there occur situations where the aggregation changes dramatically the population dynamics, from the declining original to increasing aggregate (cf. Tables 2 and 3 for $t = 2013$ in [41]). A mathematical ground for such a change does also exist (ibidem).

Reproductive uncertainty introduces certain problems into the way we associate each successive point, $\theta(k)$, $k = 1960, \dots, 2019$, of our long time series to one of the 11 reference points, i.e., to one of the 11 PPMs, the way being, ideologically, the same as before [1], but technically different. The first problem arises because of a duality in the choice of the reference PPMs, and we eliminate the duality by having recourse to a 2nd-order Markov formalism. The second problem is the set of t -specific PPMs (Table 2) instead of a single PPM in the former case (Table 2 in [1]), and we resolve the problem by taking an advantage of the integer-valued formalism and what has been found in our former studies of another species with reproductive uncertainty (see [42] and references therein). While an optimization principle to eliminate reproductive uncertainty resulted in the extreme values of uncertain reproduction rates, their accurate calculation (after colony excavation) has led, rather, to intermediate values close to the middles of the uncertainty ranges (Tables 3 and 4 in [42]). Therefore, we have used the ready middles (a° values in Table 1) as the center of a normal distribution (with the actual variance) to select a particular a from the t -specific set, i.e., a particular t -specific PPM.

Certain ranges of uncertainty in λ_1 values (Table 2) are consonant with the well- and long-known methodology of *fuzzy logic*, which might be applied to our matrix-based fuzzy time series, similar to those in controlled thermonuclear fusion [43]. That work, even if dated, represents a milestone of prediction systems based on fuzzy logic and, in particular, on matrix-based fuzzy times series.

Our former attempt to estimate λ_5 for this population of *E. caucasicum* was based on the 8-year observation data (2009–2016) and equiprobable i.i.d. choice (Table 4 in [34]); it resulted in the range (0.934156, 0.936192) (ibidem), which is apparently closer to 1 than our present (0.921158, 0.922505) (Table 4), with the span of 0.002036 (Table 4 in [34]), which is almost twice wider than our present 0.0013463 (Table 4). A logical reason for the former fact is that one of our three additional PPM sets (2017–2019) has its range of $\{\lambda_1(a)\}$ shifted strongly to the left (Table 2), while the latter is due to the Markov chain choice instead of the i.i.d.

Smaller and more reliable estimates of the stochastic growth rate mean a higher risk of population extinction because of environment disturbances, and this motivates the issue of the status that the species might have in the Red Data Books.

Note that Table 4 contains four cases where the expectation of more accurate estimates by the Markov choice fails: the range length in grey background is smaller than that under the Markov choice on the same line. These disappointing cases can be explained first by insufficient product “length”, in combination with insufficient number of realizations, and second by the effect of reproductive uncertainty, which erodes the range by the uncertainty in λ_1 s. All these cases are still observed under the ss^* i.i.d. choice, in close relation to the Markov chain, and they can hardly disprove the general tendency following M. Tillius Cicero’s “Exceptio probat regulam in casibus non exceptis”.

5. Conclusions

We expand the paradigm of stochastic growth rates for the case of reproductive uncertainty in the data and LCG using the integer-valued formalism of matrix population models. The variable environment of a local *Eritrichium caucasicum* population is now represented as a finite set of the annual PPM sets that are also finite and have certain

bounded ranges of their λ_1 uncertainty. These sets are now the objects of random choice in constructing the finite sequences of PPM products whose limit (as the number of cofactors tends to infinity) determines the stochastic growth rate λ_S . A Markov chain that governs the choice is the same as the chain that realized a long (60-member) time series of an observed weather index correlated with the variations in the annual λ_1 s. The reproductive uncertainty causes the selection of a particular PPM from a given annual PPM set to be random too, with the selection obeying a normal distribution around a certain central PPM. Altogether, this makes the random choice more realistic than the artificial i.i.d. choice (simple and popular in the literature), even when it obeys the steady-state distribution of Markov chain states. Our extensive MC simulations of the long-enough sequences illustrate the picture intuitively expected beforehand: “realistic choice of annual matrices contracts the range of λ_S estimates under reproductive uncertainty too”.

The figures obtained by the realistic choice (0.924874, 0.926079) suggest that the local population of *E. caucasicum* may decrease by 50% in 9 years under the spectrum of observed conditions, similar to what has been predicted for *Androsace albana* [1], another short-lived perennial alpine species endemic to Caucasus. The former is, however, not included into the recent regional Red Data Books, in contrast to the latter [44,45], and our findings motivate both the further monitoring of *E. caucasicum* populations and the issue of the species' inclusion into the Books.

Supplementary Materials: The following are available online at <https://www.mdpi.com/article/10.3390/math9233007/s1>, Table S1: Results of regression models for the $\lambda_1(t; a^\circ)$ series of *Eritrichium caucasicum*, Table S2: Associating each successive point, $\theta(k)$, $k = 1960, \dots, 2019$, of the temperature index time series to one of the 11 reference values.

Author Contributions: Conceptualization, D.O.L. and N.G.U.; methodology, D.O.L. and N.G.U.; software, D.O.L., L.L.G. and N.G.U.; validation, D.O.L.; formal analysis, D.O.L. and N.G.U.; investigation, D.O.L., L.L.G. and N.G.U.; resources, D.O.L. and N.G.U.; data curation, N.G.U. and E.S.K.; writing—original draft preparation, D.O.L.; visualization, D.O.L.; supervision, D.O.L.; project administration, D.O.L.; funding acquisition, D.O.L. All authors have read and agreed to the published version of the manuscript.

Funding: This research was funded by the Russian Fund for Basic Research, grant number 19-04-01227.

Acknowledgments: We thank Vladimir G. Onipchenko for valuable comments and assistance in providing meteorological data from Teberda, in cooperation with Mikhail Makarov, and Tatiana Elumeeva for her help with statistical processing of the data by means of RKWard, version 0.6.1. Further programming and calculations were implemented in the Embarcadero C++ Free Compiler 10.1.

Conflicts of Interest: The authors declare no conflict of interest. The funders had no role in the design of the study; in the collection, analyses, or interpretation of data; in the writing of the manuscript, or in the decision to publish the results.

Appendix A. Diverging/Vanishing Sequences and a Remedy to Cope with

“A finite sequence (3) of any given length” bears, in fact, a technical problem. A great enough number of cofactors in a term of sequence (3) that have their λ_1 s less than 1 causes the term to tend to zero, while a great-enough number of cofactors with λ_1 s greater than 1 causes the term to tend to infinity. The terms of both kinds do appear in a long-enough sequence constructed randomly. As a result, the sequence realization becomes diverging or vanishing, in contrast to the theoretical tenet. In a computer, this artifact expresses in the term, becoming either the computer zero or computer infinity, because of a finite number of bits in the processor bit grid (64 in modern laptops).

Our former studies [11,12] have characterized the long-term trend in *E. caucasicum* population dynamics as a slow decline, and our present computer trials have resulted in vanishing rather than diverging sequences. Therefore, to reveal the converging potential of sequence (3), we have to avoid the computer zero in our MC simulations. To do so, we scale the current term as soon as it approaches zero, i.e., becomes less than a threshold

value $z > 0$, by dividing the term by a *scaling factor* $sf < 1$, and by properly rescaling the final term of a finite sequence.

To obtain the random realizations, we use the MT19937 generator of pseudorandom numbers uniformly distributed in $(0, 1)$ [46,47] (for a 64-bit processor).

To generate normally distributed pseudorandom numbers, we use the Box–Muller transformation of uniformly distributed numbers [39].

References

- Logofet, D.O.; Golubyatnikov, L.L.; Ulanova, N.G. Realistic choice of annual matrices contracts the range of λ_S estimates. *Mathematics* **2020**, *8*, 2252. [[CrossRef](#)]
- Caswell, H. *Matrix Population Models: Construction, Analysis and Interpretation*, 2nd ed.; Sinauer Associates: Sunderland, MA, USA, 2001.
- Logofet, D.O. Projection matrices revisited: A potential-growth indicator and the merit of indication. *J. Math. Sci.* **2013**, *193*, 671–686. [[CrossRef](#)]
- Horn, R.A.; Johnson, C.R. *Matrix Analysis*; Cambridge University Press: Cambridge, UK, 1990.
- Logofet, D.O. *Matrices and Graphs: Stability Problems in Mathematical Ecology*; CRC Press: Boca Raton, FL, USA, 1993.
- Logofet, D.O.; Ulanova, N.G.; Belova, I.N. Adaptation on the ground and beneath: Does the local population maximize its λ_1 ? *Ecol. Complex.* **2014**, *20*, 176–184. [[CrossRef](#)]
- Logofet, D.O. Projection matrices in variable environments: λ_1 in theory and practice. *Ecol. Model.* **2013**, *251*, 307–311. [[CrossRef](#)]
- Logofet, D.O.; Kazantseva, E.S.; Belova, I.N.; Onipchenko, V.G. Local population of *Eritrichium caucasicum* as an object of mathematical modelling. I. Life cycle graph and a nonautonomous matrix model. *Biol. Bull. Rev.* **2017**, *7*, 415–427. [[CrossRef](#)]
- Logofet, D.O.; Kazantseva, E.S.; Belova, I.N.; Onipchenko, V.G. Local population of *Eritrichium caucasicum* as an object of mathematical modelling. II. How short does the short-lived perennial live? *Biol. Bull. Rev.* **2018**, *8*, 415–427. [[CrossRef](#)]
- Logofet, D.O. Convexity in projection matrices: Projection to a calibration problem. *Ecol. Model.* **2008**, *216*, 217–228. [[CrossRef](#)]
- Logofet, D.O.; Kazantseva, E.S.; Belova, I.N.; Onipchenko, V.G. How long does a short-lived perennial live? A modelling approach. *Biol. Bull. Rev.* **2018**, *8*, 406–420. [[CrossRef](#)]
- Logofet, D.O.; Kazantseva, E.S.; Belova, I.N.; Onipchenko, V.G. Local population of *Eritrichium caucasicum* as an object of mathematical modelling. III. Population growth in the random environment. *Biol. Bull. Rev.* **2019**, *9*, 453–464. [[CrossRef](#)]
- Tuljapurkar, S.D. *Population Dynamics in Variable Environments*; Springer: New York, NY, USA, 1990.
- Kazantseva, E.S. Population Dynamics and Seed Productivity of Short-Lived Alpine Plants in the North-West Caucasus. Candidate of Science (Biology) Dissertation, Moscow State University, Moscow, Russia, 2016. (In Russian)
- Körner, C. *Alpine Plant Life: Functional Plant Ecology of High Mountain Ecosystems*, 2nd ed.; Springer: Berlin/Heidelberg, Germany, 2003.
- Rabonov, T.A. *Life Cycle of Perennial Herbaceous Plants in Meadow Phytocoenoses*; Tr. BIN Academy of Sciences of the USSR. Geobotany. USSR Academy of Sciences: Moscow, Russia, 1950; Volume 6, pp. 7–204. (In Russian)
- Rabotnov, T.A. *Fitotsenologiya (Phytocenology)*; Moscow State University Publisher: Moscow, Russia, 1978. (In Russian)
- Bender, M.H.; Baskin, J.M.; Baskin, C.C. Age of maturity and life span in herbaceous, polycarpic perennials. *Bot. Rev.* **2000**, *66*, 311–349. [[CrossRef](#)]
- Keller, R.; Vittoz, P. Clonal growth and demography of a hemicyptophyte alpine plant: *Leontopodium alpinum* Cassini. *Alp. Bot.* **2015**, *125*, 31–40. [[CrossRef](#)]
- Nakhutsrishvili, G.S.; Gamtseimidze, Z.G. *Zhizn' Rastenii v Extremal'nykh Usloviyakh Vysokogorii: Na Primere Tsentralnogo Kavkasa (Plant Life in Extreme High Altitude Conditions by Example of the Central Caucasus)*; Nauka: Leningrad, Russia, 1984.
- Onipchenko, V.G. (Ed.) *Alpine Ecosystems in the Northwest Caucasus*; Kluwer: Dordrecht, The Netherlands, 2004.
- Furstenberg, H.; Kesten, H. Products of random matrices. *Annals Math. Stat.* **1960**, *31*, 457–469. [[CrossRef](#)]
- Oseledec, V.I. A multiplicative ergodic theorem: Ljapunov characteristic numbers for dynamical systems. *Trans. Moscow Math. Soc.* **1968**, *19*, 197–231.
- Cohen, J.E. Ergodicity of age structure in populations with Markovian vital rates, I: Countable states. *J. Am. Stat. Ass.* **1976**, *71*, 335–339. [[CrossRef](#)]
- Richardson, C.W. Stochastic simulation of daily precipitation, temperature and solar radiation. *Water Resour. Res.* **1981**, *17*, 182–190. [[CrossRef](#)]
- Johnson, G.L.; Hanson, C.L.; Hardegree, S.P.; Ballard, E.B. Stochastic weather simulation—Overview and analysis of two commonly used models. *J. Appl. Meteorol.* **1996**, *35*, 1878–1896. [[CrossRef](#)]
- Johnson, G.L.; Daly, C.; Taylor, G.H.; Hanson, C.L. Spatial variability and interpolation of stochastic weather simulation model parameters. *J. Appl. Meteorol.* **2000**, *39*, 778–796. [[CrossRef](#)]
- Dubrovsky, M.; Zalud, Z.; Stastna, M. Sensitivity of CERES–Maize yields to statistical structure of daily weather series. *Clim. Chang.* **2000**, *46*, 447–472. [[CrossRef](#)]
- Cohen, J.E. Ergodicity of age structure in populations with Markovian vital rates, II: General states. *Adv. Appl. Prob.* **1977**, *9*, 18–37. [[CrossRef](#)]

30. Sanz, L. Conditions for growth and extinction in matrix models with environmental stochasticity. *Ecol. Model.* **2019**, *411*, 108797. [[CrossRef](#)]
31. Steinsaltz, D.; Tuljapurkar, S.; Horvitz, C. Derivatives of the stochastic growth rate. *Theor. Popul. Biol.* **2011**, *80*, 1–15. [[CrossRef](#)]
32. Morris, W.F.; Tuljapurkar, S.; Haridas, C.V.; Menges, E.S.; Horvitz, C.C.; Pfister, C.A. Sensitivity of the population growth rate to demographic variability within and between phases of the disturbance cycle. *Ecol. Lett.* **2006**, *9*, 1331–1341. [[CrossRef](#)] [[PubMed](#)]
33. Rees, M.; Ellner, S.P. Integral projection models for populations in temporally varying environments. *Ecol. Monogr.* **2009**, *79*, 575–594. [[CrossRef](#)]
34. Logofet, D.O. Does averaging overestimate or underestimate population growth? It depends. *Ecol. Model.* **2019**, *411*, 108744. [[CrossRef](#)]
35. Shapiro, S.S.; Wilk, M.B. An analysis of variance test for normality (complete samples). *Biometrika* **1965**, *52*, 591–611. [[CrossRef](#)]
36. Pinheiro, J.; Bates, D.; DebRoy, S.; Sarkar, D.; R Core Team. nlme: Linear and Nonlinear Mixed Effects Models. R Package Version 3.1-128. Available online: <http://CRAN.R-project.org/package=nlme> (accessed on 20 October 2021).
37. R Core Team. *R: A Language and Environment for Statistical Computing*; R Foundation for Statistical Computing: Vienna, Austria, 2016. Available online: <https://www.R-project.org/> (accessed on 20 October 2021).
38. Kemeny, J.G.; Snell, J.L. *Finite Markov Chains*; Van Nostrand: Princeton, NJ, USA, 1960.
39. Box, G.E.P.; Muller, M.E. A Note on the generation of random normal deviates. *Ann. Math. Stat.* **1958**, *29*, 610–611. [[CrossRef](#)]
40. Logofet, D.O.; Kazantseva, E.S.; Onipchenko, V.G. Seed bank as a persistent problem in matrix population models: From uncertainty to certain bounds. *Ecol. Model.* **2020**, *438*, 109284. [[CrossRef](#)]
41. Logofet, D.O. Aggregation may or may not eliminate reproductive uncertainty. *Ecol. Modell.* **2017**, *363*, 187–191. [[CrossRef](#)]
42. Logofet, D.O.; Ulanova, N.G.; Belova, I.N. From uncertainty to an exact number: Developing a method to estimate the fitness of a clonal species with polyvariant ontogeny. *Biol. Bull. Rev.* **2017**, *7*, 387–402. [[CrossRef](#)]
43. Versaci, M.M.; Morabito, F.C. Fuzzy time series approach for disruption prediction in Tokamak reactors. *IEEE Trans. Magn.* **2003**, *39*, 1503–1506. [[CrossRef](#)]
44. Zamotaylov, A.S. (Ed.) *Red Book of the Adygea Republic: Rare and Endangered Objects of Fauna and Flora. In 2 Parts, Part 1: Plants and Fungi*, 2nd ed.; Kachestvo: Maykop, Russia, 2012. (In Russian)
45. Litvinskaya, S.A. (Ed.) *Red Book of the Krasnodar Territory (Plants and Mushrooms)*, 3rd ed.; Design Bureau No. 1: Krasnodar, Russia, 2017. (In Russian)
46. Matsumoto, M.; Nishimura, T. Mersenne twister: A 623-dimensionally equidistributed uniform pseudo-random number generator. *ACM Trans. Model. Comput. Simul.* **1998**, *8*, 3–30. [[CrossRef](#)]
47. Nishimura, T. Tables of 64-bit Mersenne twisters. *ACM Trans. Model. Comput. Simul.* **2000**, *10*, 348–357. [[CrossRef](#)]